THE JOURNAL OF PHYSICAL CHEMISTRY B

Article

pubs.acs.org/JPCB

Temperature Effect on Dual Fluorescence of 2-(2′-Hydroxyphenyl)benzimidazole and Its Nitrogen Substituted Analogues

Francis A. S. Chipem and Govindarajan Krishnamoorthy*

Department of Chemistry, Indian Institute of Technology Guwahati, Guwahati 781 039, India

Supporting Information

ABSTRACT: The effects of temperature on the dual fluorescence of 2-(2′-hydroxyphenyl)benzimidazole (HPBI) and its nitrogen substituted analogues, viz., 2-(2′-hydroxyphenyl)-3*H*-imidazo[4,5-*b*]pyridine (HPIP-b) and 2-(2′-hydroxyphenyl)-1*H*-imidazo[4,5-*c*]pyridine (HPIP-c), were investigated in solvents of different polarity and hydrogen bonding capability. Absorption, steady-state, and time-resolved emission spectroscopic techniques were employed for the experimental study. Density functional theoretical calculations were performed to find the relative population of the conformers. The calculations predict that, with increase in temperature, the population of *trans*-enol increases, while that of *cis*-enol decreases. At all temperatures, the population ratio of *cis*-enol to *trans*-enol increases in the order HPIP-c < HPIP-b < HPBI. Except for HPBI in methanol and ethylene glycol, the fluorescence of both emissions decreases with an increase in temperature and is more pronounced in the tautomer band than in the normal band. The data are analyzed using the Arrhenius and van't Hoff equations. The change in the fluorescence with temperature is governed by (i) the change in the relative population of conformers and (ii) the increase in non-radiative decay from the excited states. The increase in non-radiative decay from the normal emission competes with the increase in the relative population of *trans*-enol with a rise in temperature.

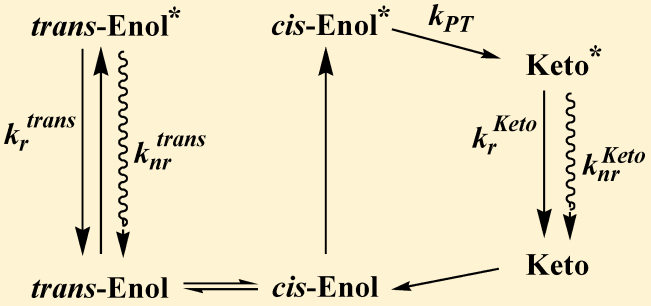

1. INTRODUCTION

Proton transfer reactions play a vital role in a variety of chemical and biological processes and have been extensively investigated.[1,2] Among the various types of proton transfers, excited-state intramolecular proton transfer (ESIPT) has been drawing increasing attention during these past few decades, as their properties facilitate novel optoelectronic applications.[3−7] ESIPT is a phototautomerization which occurs in the excited state through an intramolecular hydrogen bonded ring. In the ESIPT process, a proton/hydrogen atom is transferred to an electronegative atom at a sub-picosecond time scale. ESIPT exhibiting molecules show dual fluorescence in which the shorter wavelength emission is called the normal emission and the highly Stokes shifted emission is called the tautomer emission. These molecules exhibit photochromism where a chemical species is transformed reversibly between two states of different excitation wavelengths due to changes in their geometrical and electronic structures.[8] Therefore, these molecules have potential implications in making memories and switches at a molecular level.[9] In addition, ESIPT molecules are used in varied fields such as fluorescence probes,[10] sensors,[6,11] lasers,[12] photostabilizers,[13] optical devices,[14] and information processing.[15]

2-(2′-Hydroxyphenyl)benzimidazole (HPBI, Chart 1) and its analogues form an interesting class of ESIPT exhibiting molecules and are studied extensively.[16−20] They find applications as lasers,[21] sensors,[4,22] and molecular switches.[15] The photophysics of these molecules are greatly affected by the environment.[19,20,23] Spectral tuning can be achieved by substitution.[4,24] The quantum yields of 2-(2′-hydroxyphenyl)-benzoxazole and 2-(2′-hydroxyphenyl)benzothiazole were reported to decrease with a rise in temperature.[18] The decrease in the quantum yield has been associated with the temperature dependent radiationless deactivation of the phototautomer. However, the mechanism of the deactivation process is still not clear.[3,25−27] It was predicted that *cis*−*trans* isomerization of the phototautomer may cause thermally activated decay through the formation of the intramolecular charge transfer (ICT) state having a twisted tautomer structure.[18,26−30] The torsional induced ICT process was observed in HPBI and its nitrogen substituted analogues, 2-(2′-hydroxyphenyl)-3*H*-imidazo[4,5-*b*]pyridine (HPIP-b, Chart 1) and 2-(2′-hydroxyphenyl)-3*H*-imidazo[4,5-*c*]pyridine (HPIP-c, Chart 1) also.[31,32]

HPBI and its nitrogen substituted analogues can exist as *cis*-enol, *trans*-enol, and *open*-enol conformers and keto tautomeric form (Chart 1). In addition, as reported by Rodríguez et al., three other conformers corresponding to the NH group in position *anti* to the N atom are possible.[33] The intramolecular

Received: June 12, 2013
Revised: October 14, 2013
Published: October 16, 2013

dx.doi.org/10.1021/jp405804c | *J. Phys. Chem. B* 2013, 117, 14079−14088

Chart 1. Different Conformeric Forms of HPBI and Its Nitrogen Substituted Analogues

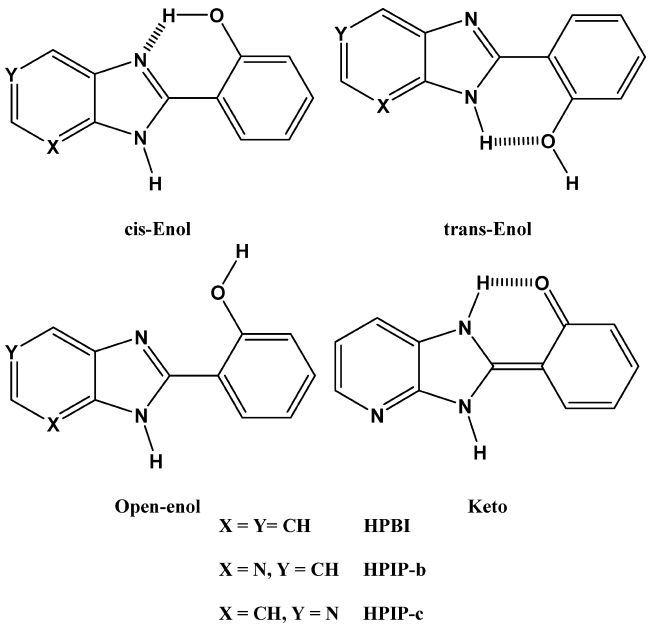

hydrogen bond between the −OH group and imidazole nitrogen is the prerequisite for the formation of a keto form in the excited state. Upon photoexcitation, the *trans*- and *open*-enol emit normal emission and *cis*-enol undergoes ESIPT to form a tautomer. The emission occurs from the tautomer. The relative population of the enol depends upon the polarity and hydrogen bonding capacity of the solvents. In other words, the relative intensities of the normal and tautomer bands depend on the nature of the environment. The fluorescence ratio of the normal to the tautomer emissions is enhanced in protic solvent compared to those in aprotic solvents. Although the spectral characteristics of HPBI, HPIP-b, and HPIP-c were investigated earlier,[19,34−37] the effects of temperature on the dual fluorescence and related photophysical processes were not reported. Literature reports suggest that the ICT process of bichromophoric molecules is affected by temperature.[38,39] In addition, the temperature affects the solvent−solute interaction and relative population of the conformer. Hence, we studied the effects of temperature on spectral characteristics of HPBI and its nitrogen substituted analogues, viz., HPIP-b and HPIP-c. In this work, the effects of temperature on the photophysics of all three molecules are investigated in non-polar solvents cyclohexane and dioxane, polar aprotic solvent acetonitrile, and protic solvents ethylene glycol and methanol.

2. MATERIALS AND METHODS

2.1. Experimental Section. The synthetic procedures of HPBI, HPIP-b, and HPIP-c were reported elsewhere.[19,35,37] The compounds were recrystallized four times in methanol before use. Acetonitrile, cyclohexane, dioxane, and methanol were of HPLC grade and were procured from Spectrochem India. Ethylene glycol (analytical grade) was obtained from Rankem India. The concentrations of the fluorophores in the solutions were maintained at ∼5 μM. UV−visible absorption spectra were recorded on a Varian Cary 100 spectrophotometer. Fluorescence emission and excitation spectra were recorded on an Edinburgh instrument FSP-920 fluorimeter. The 3D spectra at room temperature were recorded with a Jobin Yvon FluoroMax 4 instrument. Due to poor solubility of HPIP-c in cyclohexane, HPIP-c's spectra were not recorded in cyclohexane. The dielectric constants and refractive indices of different solvents at different temperatures were obtained from the literature.[40,41] Fluorescence decays were measured on an Edinburgh instruments LifeSpec II time correlated single photon counting instrument. A PicoQuant 308 nm LED with a pulse width of 635 ps was used as the light source. The decays were measured at band maximum with a 20 nm band-pass. Time-resolved data were analyzed with the reconvolution method on the basis of a discrete components analysis model using the FAST software developed by the Edinburgh Instruments. The goodness of fit was determined by the reduced χ^2 values and weighted residuals which were between the ranges of 1 ± 0.15 and ± 6, respectively. The absorption and fluorescence spectra are corrected for the variation of density with temperature, in other words for the change in the concentration of the fluorophores with temperature.

2.2. DFT Calculations. The ground state molecular geometries were fully optimized in different studied solvents at different temperatures using the integral equation formalism-polarizable continuum (IEF-PCM) model[42,43] at density functional theory level. The convergence threshold for the energies and residual forces on the atoms during geometry optimization were maintained at 10^{-8} hartree and 4.5×10^{-4} hartree/bohr, respectively. The hybrid functional B3LYP[44−47] with Pople's basis set 6-31G(d,p) was used for the calculations. Energy correction over the optimized geometries at a given temperature and solvent was performed by using the 6-31+G(d,p) basis set with the same method and solvation model to take into account diffuse functions as a result of hydrogen bonding. The dielectric constants of the solvents at a given temperature (from the literature)[40] were used for every calculation. All the computations were carried out using a developed version of Gaussian 03.[48]

3. RESULTS AND DISCUSSION

3.1. Population Ratio of Enol Conformers. The population ratios of *cis*-enol to *trans*-enol at different temperatures for all three molecules are plotted (Figure S1a, Supporting Information) using the Boltzmann distribution equation (eq 1)

Chart 2. Different Solvated Structures of HPBI Considered in the Calculations

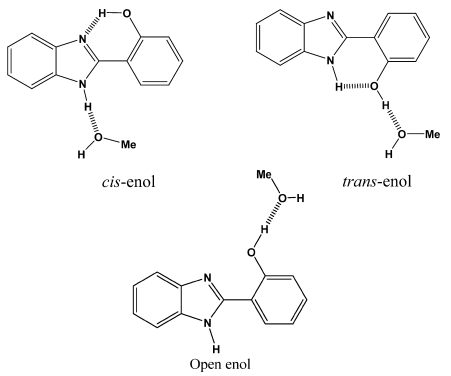

$$\frac{N_{cis}}{N_{trans}} = e^{-\Delta E/kT} \quad (1)$$

dx.doi.org/10.1021/jp405804c | J. Phys. Chem. B 2013, 117, 14079−14088

Chart 3. Different Solvated Structures of HPIP-b Considered in the Calculations

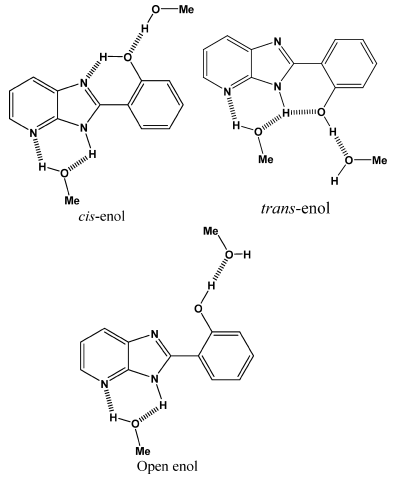

Chart 4. Different Solvated Structures of HPIP-c Considered in the Calculations

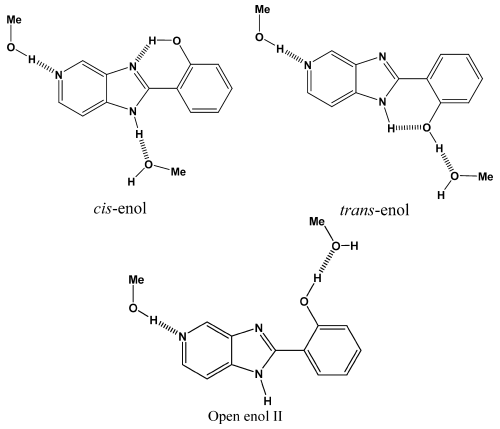

The population ratios of *trans*-enol to *open*-enol at different temperatures are given as Supporting Information (Figure S1b). The relative population of *open*-enol is negligible and at any given temperature and solvent. However, as the temperature increases, the relative population of *open*-enol with respect to other enols increases. It decreases in the order HPBI > HPIP-b > HPIP-c. For all of the molecules in all of the solvents, the ratio decreases with an increase in temperature, which indicates that the population of *trans*-enol relative to *cis*-enol increases. In other words, the *trans*-enol becomes more favorable with an increase in temperature.

In the IEF-PCM solvation model, the role of specific interaction between the solvent and solute molecules through hydrogen bonding was not considered. However, specific hydrogen bonding between the solvent and the solute molecules will result in a solvated form (Charts 2–4). Such a hydrogen bonding significantly affects the relative population of different enol forms in protic solvents. To take into account the effect of hydrogen bonding, as a representation, optimizations were carried out by adding one methanol molecule to HPBI and two methanol molecules to HPIP-b and HPIP-c molecules. The relative population of *open*-enol and *trans*-enol increases greatly compared to *cis*-enol (Figure S2, Supporting Information). This is due to the hydrogen bonding in solvated structures. Although the relative stability of *open*-enol is enhanced by addition of solvent molecule, still it is less than the other two enols. However, solvated *trans*-enol is more stable than solvated *cis*-enol in HPIP-b.

3.2. Absorption Spectra. The absorption spectra of HPBI, HPIP-b, and HPIP-c in all the solvents consist mainly of three bands at 285–300, 315–325, and 330–340 nm (Figures S3.1–S3.3, Supporting Information). The absorption spectra of HPBI and HPIP-b are more structured than those of HPIP-c. In a given solvent and at the same temperature, the absorption peaks are red-shifted in HPIP-b compared to HPIP-c which are red-shifted compared to HPBI.

The absorption spectra of HPBI, HPIP-b, and HPIP-c in all the solvents show a hypochromic effect with an increase in temperature with the exception of HPIP-b in cyclohexane. Peculiar behavior is observed for the absorption spectra of HPIP-b in cyclohexane: the absorbance decreases with a blue shift for an initial increase in temperature from 283 to 323 K. However, upon further increase of temperature from 323 to 348 K, the absorbance increases without any shift. In most cases, the absorption maxima remain insensitive to the change in temperature. However, like the spectra of HPIP-b in cyclohexane, a small blue shift is observed in those of HPBI and HPIP-b in ethylene glycol.

3.3. Fluorescence Emission Spectra. At room temperature, all three molecules emit dual fluorescence in most of the

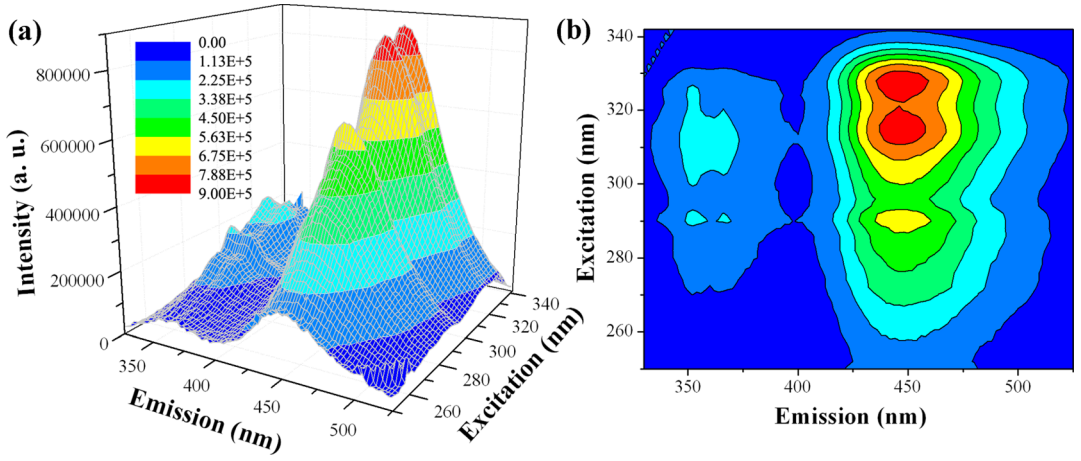

Figure 1. (a) 3-D emission spectra of HPIP-c in methanol at room temperature and (b) its corresponding contour diagram.

dx.doi.org/10.1021/jp405804c | J. Phys. Chem. B 2013, 117, 14079–14088

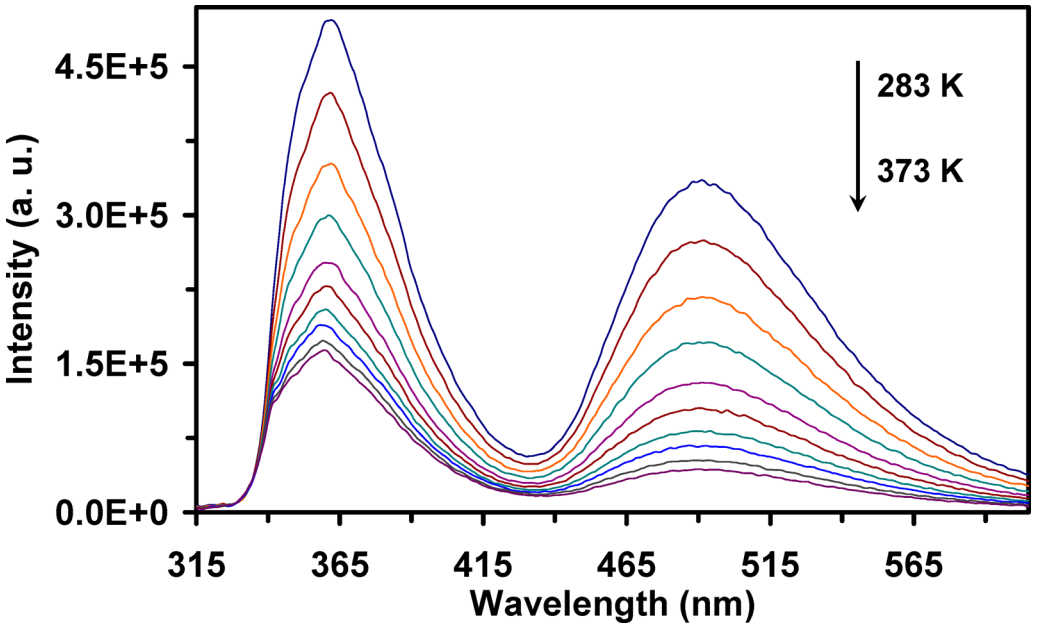

Figure 2. Emission spectra of HPIP-b in ethylene glycol at different temperatures (λ_{exc} = 310 nm).

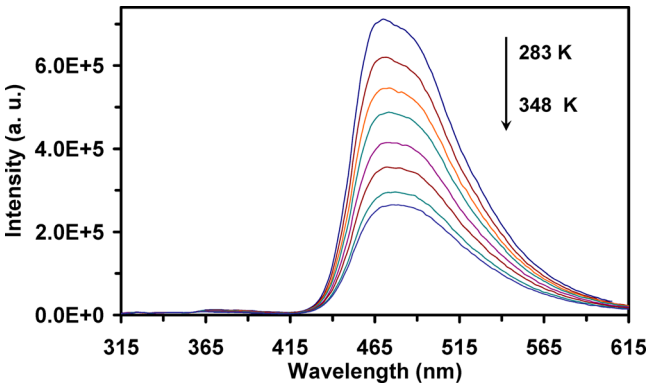

Figure 3. Emission spectra of HPBI in cyclohexane at different temperatures (λ_{exc} = 310 nm).

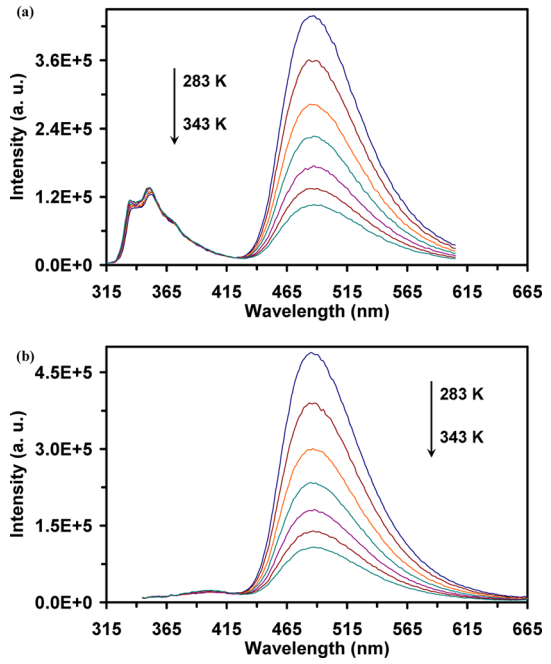

Figure 4. Emission spectra of HPIP-b in acetonitrile at different temperatures excited at (a) 310 nm and (b) 340 nm.

solvents. As mentioned earlier, the shorter wavelength emission band that exhibits vibrational structure is due to normal emission from the excited *trans*-enol. The red-shifted intense emission band is due to emission from the keto form by ESIPT. It is characterized by its large Stokes shift from the absorption band.[19,35−37,49,50] The relative fluorescence intensities of the bands depend on the wavelength of excitation. It is illustrated by the representative 3D emission spectra and the corresponding contour diagram of HPIP-c in methanol at room temperature (Figure 1). All three molecules emit clear dual fluorescence in protic solvents. The normal emissions are more intense than the tautomer emissions of HPIP-b and HPIP-c in both methanol and ethylene glycol (representative plot is presented as Figure 2). On the other hand, the tautomer emissions dominate over the normal emissions in aprotic solvents. HPBI shows almost a single emission from keto form in cyclohexane with negligible normal emission (Figure 3). Upon increasing the polarity and hydrogen bonding capacity of the solvents, the normal bands of all three molecules are red-shifted and the keto bands of HPBI and HPIP-c are blue-shifted. However, the keto band of HPIP-b is insensitive to the solvent effect. All of these results are consistent with the earlier literature reports.[19,35−37]

The emission band maxima of both normal and tautomer emission are independent of excitation wavelength in aprotic solvents. As a representative, the emission spectra of HPIP-b in acetonitrile at different temperatures at two different excitations are shown in Figure 4. This shows that emissions occur from excited state structures of completely relaxed states at this range of temperatures. However, upon exciting at different wavelength, a small shift is observed in the fluorescence spectra of pyridyl nitrogen substituted molecules in protic solvents. Figure 5 shows the normalized emission spectra of HPIP-b in methanol as a representative plot. This may be due to the

dx.doi.org/10.1021/jp405804c | J. Phys. Chem. B 2013, 117, 14079−14088

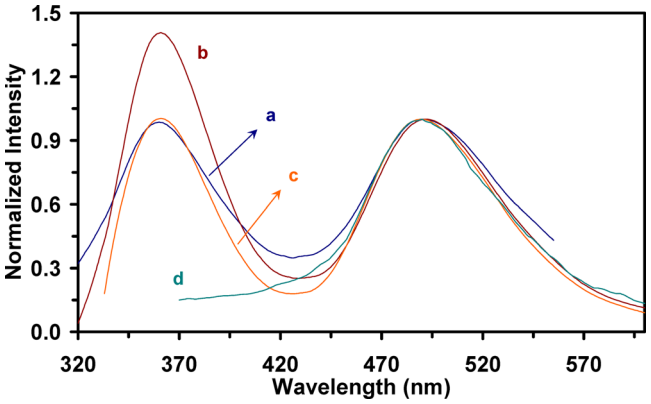

Figure 5. Normalized fluorescence spectra of HPIP-b in methanol with respect to the normal emission band: λ_{exc} = (a) 280 nm, (b) 310 nm, (c) 330 nm, and (d) 350 nm.

presence of different solvated structures (discussed later in section 3.4). The variation in temperature hardly affects the emission band position (Table S1 and Figure S4, Supporting Information). However, it affects the fluorescence intensities and the magnitude of the effect depends upon the nature of the solvent. The fluorescence spectra of HPIP-b in acetonitrile (Figure 4) and HPIP-b in ethylene glycol (Figure 2) are representations to demonstrate the effect of temperature in aprotic and protic solvents, respectively. In aprotic solvents where the normal emissions are weak, the temperature effects on their spectral intensities are relatively smaller, but the strong tautomer emission intensity decreases significantly with a rise in temperature. However, in protic solvents where the normal emission is significant, both tautomer and normal emissions decrease substantially with an increase in temperature. As discussed earlier, the *cis*-enol, which forms an intramolecular hydrogen bonded cyclic ring, is the species responsible for ESIPT and *trans*-enol is responsible for the normal emission.[19,35−37] The breaking of an intramolecular hydrogen bond in *cis*-enol by protic solvents increases the relative population of *trans*-enol which increases the normal emission in methanol and ethylene glycol. In glycol, the fluorescence increases further due to the higher viscosity of the medium. The decrease in fluorescence intensities of the tautomer emission with increase in temperature is more than those of normal emission. The difference in the decrease between normal and tautomer emission intensities is less in protic solvents than in aprotic solvents.

The fluorescence of the normal band of both HPBI and HPIP-b in acetonitrile and dioxane increases with an increase in temperature (Figures S4 and S5, Supporting Information). This increase in fluorescence of normal emission with a rise in temperature is due to the increase in the population of *trans*-enol in the ground state as predicted by the theoretical calculations. On the other hand, the fluorescence intensity of the normal emission of HPIP-c in acetonitrile remains almost constant and a very small decrease is observed in dioxane. This difference in behavior of HPIP-c can be explained by the fact that the relative population of *trans*-enol to *cis*-enol decreases in the order HPBI > HPIP-b > HPIP-c. The quantum yields of the normal bands of all three molecules in protic solvents and those of HPBI and HPIP-b in cyclohexane decrease with a rise in temperature. Although initially a negative slope is exhibited for the variation of the normal fluorescence of HPBI with temperature in methanol, and those of both HPIP-b and

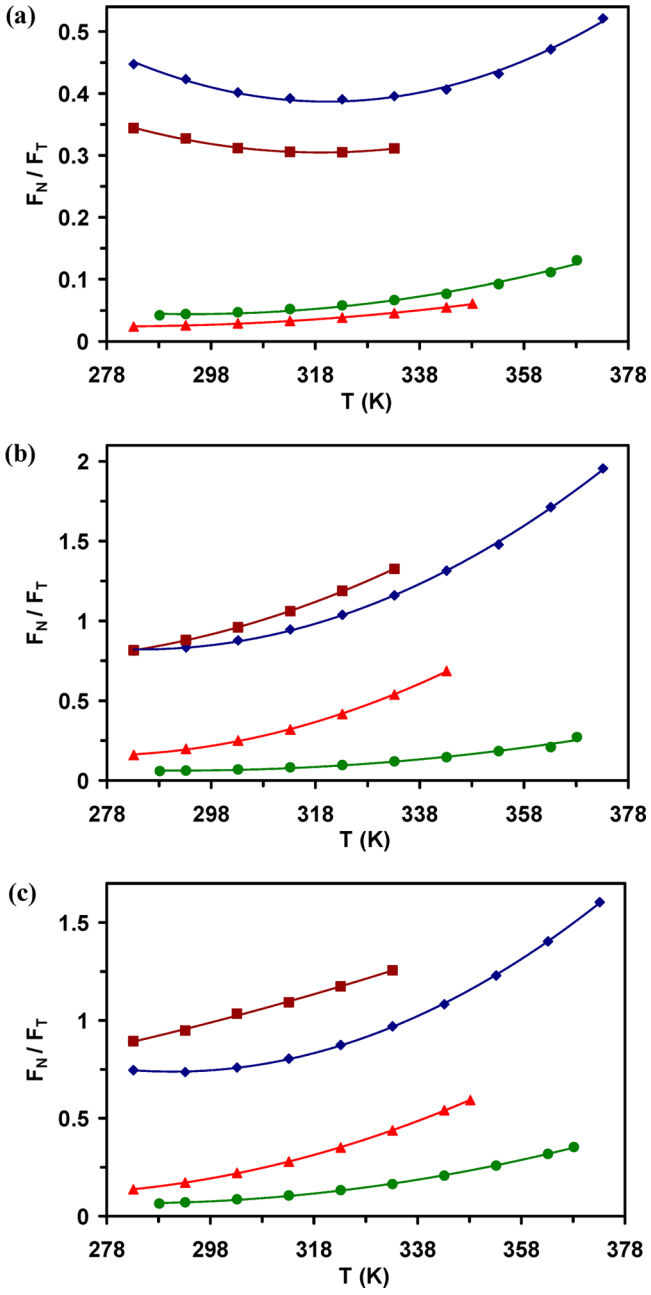

Figure 6. Fluorescence ratio of normal to tautomer bands of (a) HPBI, (b) HPIP-b, and (c) HPIP-c in dioxane (green ●), acetonitrile (red ▲), methanol (maroon ■), and ethylene glycol (blue ◆) at different temperatures (λ_{exc} = 310 nm).

Table 1. Enthalpy Difference (ΔH, cal/mol) between *trans*-Enol and *cis*-Enol in Different Molecules in Different Solvents

	ΔH		
solvent	HPBI	HPIP-b	HPIP-c
1,4-dioxane	2836	3895	4520
acetonitrile	2832	2377	4476
methanol		1827	1281
ethylene glycol		2083	1847

HPIP-c in ethylene glycol, the plots are curved upward at higher temperature. On the other hand, the fluorescence intensity of the tautomer bands of all molecules decreases with

dx.doi.org/10.1021/jp405804c | J. Phys. Chem. B 2013, 117, 14079−14088

Table 2. Fluorescence Lifetime of HPBI in Different Studied Solvents at Different Temperatures[a]

	cyclohexane		1,4-dioxane		acetonitrile		methanol		ethylene glycol	
temperature (K)	τ^N	τ^T	τ^N	τ^T	τ^N	τ^T	τ^N	τ^T	τ^N	τ^T
293	1.74	3.76	1.41	4.32	1.58	3.83	1.59	3.93	1.62	4.48
303	1.71	3.52	1.33	4.15	1.59	3.62	1.58	3.82	1.61	4.31
313	1.71	3.29	1.34	3.96	1.65	3.39	1.56	3.72	1.60	4.12
323	1.68	3.06	1.38	3.72	1.68	3.14	1.60	3.63	1.60	3.89
333	1.62	2.80	1.38	3.58	1.71	2.92	1.63	3.48	1.59	3.67
343	1.60	2.51	1.37	3.35	1.78	2.65			1.59	3.39

[a]Lifetimes are given in nanoseconds.

Table 3. Fluorescence Lifetime of HPIP-b in Different Studied Solvents at Different Temperatures[a,b]

	cyclohexane[c]	1,4-dioxane		acetonitrile		methanol				ethylene glycol		
temperature (K)	τ^T	τ^N	τ^T	τ^N	τ^T	τ_1^N (f_1)	τ_2^N (f_2)	τ_1^T (f_1)	τ_2^T (f_2)	τ_1^N (f_1)	τ_2^N (f_2)	τ^T (f_1)
293	3.41	1.02	3.66	1.14	1.59	0.55 (32)	1.65 (68)	0.84 (80)	4.47 (20)	0.64 (89)	2.35 (11)	2.00
303	3.02	1.00	3.28	1.10	1.33	0.76 (41)	1.69 (59)	0.70 (81)	4.35 (19)	0.55 (86)	2.28 (14)	1.52
313	2.62	0.99	2.82	1.09	1.00	0.71 (43)	1.69 (57)	0.58 (78)	4.34 (22)	0.53 (86)	2.31 (14)	1.24
323	2.26	0.96	2.46	1.07	0.82	0.52 (34)	1.63 (66)	0.45 (74)	4.24 (26)	0.42 (79)	1.88 (21)	0.97
333	1.89	0.96	2.12	1.04	0.67	0.51 (34)	1.68 (66)	0.39 (72)	4.14 (28)	0.42 (79)	1.91 (21)	0.78
343	1.56	0.95	1.66	1.04	0.58					0.39 (75)	1.77 (25)	0.64

[a]Lifetimes are given in nanoseconds. [b]Values within parentheses are the relative amplitudes of the component. [c]The lifetime of the normal species could not be measured due to weak fluorescence of the normal species.

Table 4. Fluorescence Lifetime of HPIP-c in Different Studied Solvents at Different Temperatures[a,b]

	1,4-dioxane		acetonitrile		methanol				ethylene glycol	
temperature (K)	τ^N	τ^T	τ^N	τ^T	τ_1^N (f_1)	τ_2^N (f_2)	τ_1^T (f_1)	τ_2^T (f_2)	τ^N	τ^T
293	1.10	2.85	1.28	1.45	0.32 (84)	1.84 (16)	0.98 (86)	3.10 (14)	0.79	2.36
303	1.06	2.36	1.26	1.12	0.29 (84)	1.87 (16)	0.77 (86)	3.24 (14)	0.68	1.81
313	1.04	2.16	1.24	0.88	0.32 (85)	2.12 (16)	0.62 (86)	3.42 (14)	0.60	1.39
323	1.03	1.69	1.22	0.71	0.26 (84)	2.34 (16)	0.49 (84)	3.46 (16)	0.50	1.13
333	1.01	1.50	1.21	0.62	0.29 (84)	2.91 (16)	0.44 (83)	3.54 (17)	0.45	0.88
343	0.97	1.44	1.20	0.49					0.41	0.60

[a]Lifetimes are given in nanoseconds. [b]Values within parentheses are the relative amplitudes of the component.

an increase in temperature in all of the solvents (Figure S6, Supporting Information). This is due to a decrease in the relative population of *cis*-enol and enhanced non-radiative decay of the keto-tautomer with an increase in temperature. Our earlier theoretical calculations predicted that the torsional rotation of the keto-tautomer to a twisted ICT state acts as a non-radiative channel in HPBI and its analogues.[31,32] The calculations also predicted that the ICT process is more favored upon nitrogen substitution and is consistent with smaller quantum yields of HPIP-b and HPIP-c than that of HPBI. Rodríguez et al. reported that different prototropic species of HPIP-b undergo efficient radiationless deactivation through a twisted ICT channel.[33] Further, they found that the methylated derivative of HPIP-b at pyridine nitrogen is non-fluorescent due to the formation of a non-emissive ICT state after ESIPT.[51] The methylation enhances the electron withdrawing ability of the azole moiety, and hence, the ICT from the phenolic moiety to the heterocyclic ring is more favored. More recently, Sekiya et al. demonstrated the polymorphic dependent photophysics of HPBI.[34] They reported the formation of a twisted conformer of HPBI in its polymorphs as a result of ESIPT followed by ICT. Further, they proposed that the decrease in quantum yield is associated with ICT. The rise in temperature is expected to favor the twisting motion and thereby enhance the formation of a non-emissive ICT state. Kim et al. showed that the ESIPT through the intramolecular hydrogen bond lowers the activation energy for ICT in *p-N,N*-dimethylaminosalicylic acid.[52]

The fluorescence (spectral area) ratios (F_N/F_T) of normal to tautomer bands of HPBI, HPIP-b, and HPIP-c in different solvents at different temperatures are shown in Figure 6. At a given temperature, the ratio of HPIP-b and HPIP-c is in the order methanol > ethylene glycol > acetonitrile > dioxane. The trend is in correlation with the calculated population ratios of *cis*-enol to *trans*-enol as discussed in section 3.1. For HPBI, it follows the order ethylene glycol > methanol > dioxane > acetonitrile. There is an increase in F_N/F_T ratio for all the molecules in all the solvents except that of HPBI in methanol and ethylene glycol where normal emission dominates over the tautomer emission. The F_N/F_T ratio of HPBI in methanol and ethylene glycol indicates that the non-radiative decay from solvated enol dominates until 323 K and above that the ratios show upward curvature.

Since F_N/F_T is the ratio of the fractional contribution, the following van't Hoff equation (eq 2) may be applied

$$R \ln\left(\frac{F_N}{F_T}\right) = R \ln\left(\frac{\phi_N \varepsilon_{trans}}{\phi_T \varepsilon_{cis}}\right) + \Delta S - \frac{\Delta H}{T} \quad (2)$$

Here ε_{trans} and ε_{cis} are the molar extinction coefficients of *trans*- and *cis*-enol conformers, respectively. ϕ_N and ϕ_T are the fluorescence quantum yields of the normal and tautomer

dx.doi.org/10.1021/jp405804c | J. Phys. Chem. B 2013, 117, 14079−14088

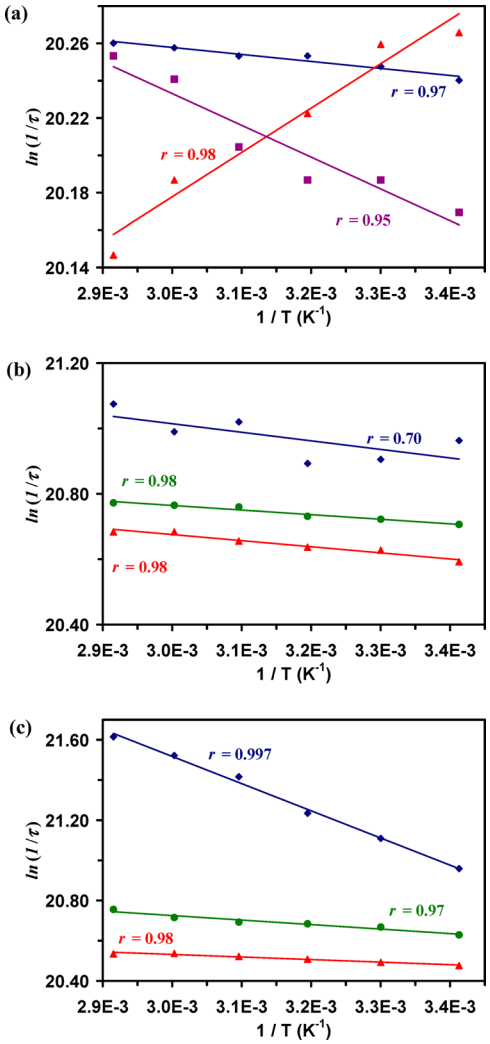

Figure 7. Arrhenius plots for normal emissions of (a) HPBI, (b) HPIP-b, and (c) HPIP-c in cyclohexane (purple ■), dioxane (green ●), acetonitrile (red ▲), methanol (maroon ■), and ethylene glycol (blue ◆) at different temperatures.

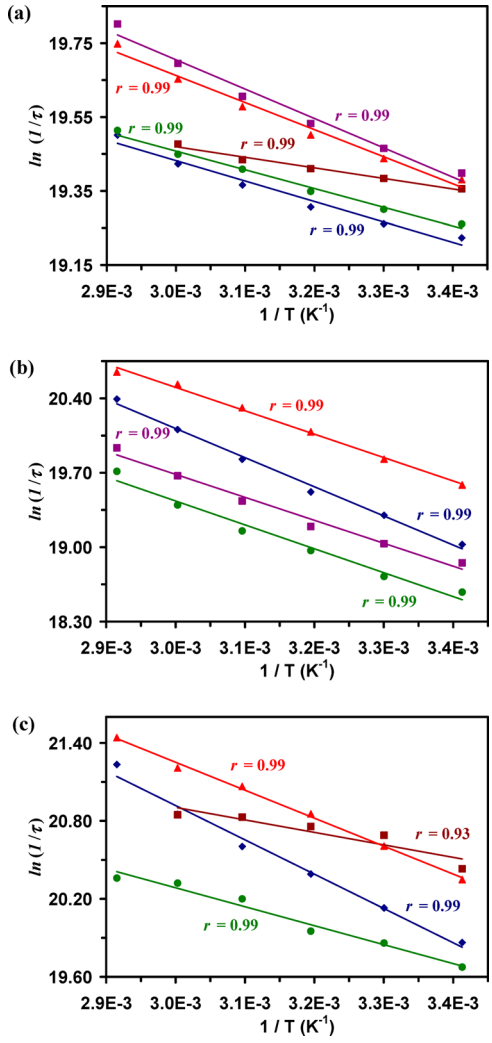

Figure 8. Arrhenius plots for tautomer emissions of (a) HPBI, (b) HPIP-b, and (c) HPIP-c in cyclohexane (purple ■), dioxane (green ●), acetonitrile (red ▲), methanol (maroon ■), and ethylene glycol (blue ◆) at different temperatures.

emission, in other words corresponding fluorescence quantum yields of two conformers, respectively, and ΔS and ΔH are the entropy and enthalpy differences between the two conformers. As expected, poor correlation is obtained for HPBI in methanol and ethylene glycol (Figure S7, Supporting Information). In all other cases, better linear correlation was obtained with a correlation coefficient of $r > 0.92$. The ΔH values, thus obtained, are compiled in Table 1. As predicted, the enthalpy difference decreases in protic solvents compared to aprotic solvents.

The excitation spectra recorded at the normal band (~350–370 nm) are blue-shifted from those recorded at the keto tautomer band (~450–495 nm) of all three molecules in all solvents (Figures S8 and S9, Supporting Information). This is consistent with the fact that the normal and tautomer emissions originate from two distinct ground state species, viz., *trans*-enol and *cis*-enol, respectively. The spectra monitored at the tautomer band match better with the corresponding absorption spectra, indicating that the species responsible for the tautomer band, i.e., the *cis*-enol, is the prominent structure in the ground state. Both excitation spectra differ considerably in aprotic solvents, but the differences in spectra are small in protic solvents due to solvation in protic solvents.

As anticipated, the effects of temperature on the excitation spectra of the normal and tautomer emissions are the same as those of respective emission spectra; i.e., the excitation spectral intensities of the tautomer band decrease in all of the solvents. The excitation spectral intensities of the normal emission vary depending on the increase in relative population of its ground state precursor and the increase in non-radiative decay with increase in temperature.

3.4. Time Resolved Fluorescence. The lifetime values of all three molecules in different solvents at different temperatures are given in Tables 2–4. Small differences are observed between the present measurements and the earlier literature values.[20,35−37] The decay of the normal emission of HPBI is less sensitive to the variation in temperature. With a rise in temperature, a small decrease in lifetimes of the normal emission of HPBI is observed in cyclohexane, dioxane, and ethylene glycol, whereas a small increase is observed in acetonitrile. The increase in lifetime of the normal emission in acetonitrile corroborates with the increase in quantum yield. However, the lifetimes of the keto tautomer of HPBI gradually

dx.doi.org/10.1021/jp405804c | J. Phys. Chem. B 2013, 117, 14079−14088

Table 5. Activation Energy (E_a, kcal/mol) and the Pre-Exponential Factor (A) Obtained from the Arrhenius Plots

	normal emission		tautomer emission	
solvent	ln A	E_a	ln A	E_a
		HPBI		
cyclohexane	20.745	−338.70	22.089	−1578.77
1,4-dioxane			20.978	−1006.83
acetonitrile	19.465	472.21	21.859	−1455.06
methanol	20.042	132.48	20.326	−567.29
ethylene glycol	20.371	−74.64	21.088	−1096.88
		HPIP-b		
cyclohexane	19.470	−92.33	26.166	−4292.71
1,4-dioxane	21.186	−279.19	26.185	−4471.35
acetonitrile	21.235	−370.56	27.117	−4380.14
methanol			21.293	
ethylene glycol	21.800	−519.98	28.341	−5447.16
		HPIP-c		
1,4-dioxane	21.401	−447.25	24.658	−2896.05
acetonitrile	20.914	−253.7	27.704	−4273.84
methanol			23.784	−1907.78
ethylene glycol	25.575	−2687.62	28.839	−5246.08

Scheme 1. Kinetics Schemes for the Decay of *trans*-Enol and ESIPT Process of HPBI and Its Nitrogen Substituted Analogues

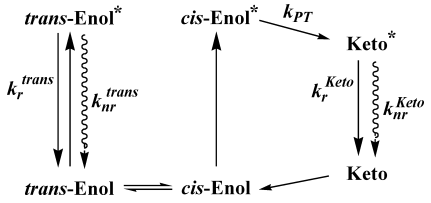

decrease with an increase in temperature in all of the solvents. The decrease in lifetime of the phototautomer indicates the enhanced non-radiative deactivation. The rise in temperature has a greater effect on the lifetimes of the tautomer than that of normal species.

In ethylene glycol, the tautomer emissions of both HPIP-b and HPIP-c are single exponential. The normal emission of HPIP-c is monoexponential and that of HPIP-b is biexponential. On the other hand, the normal and tautomer emissions of both HPIP-b and HPIP-c are single exponentials in all aprotic solvents. However, the decay in methanol is biexponential. This suggests that due to the presence of pyridyl nitrogen the local environment around pyridyl nitrogen substituted analogues has different solvation in protic solvents and thus a different lifetime. Dogra et al. have also suggested the presence of different solvated forms in protic solvents.[19,35−37] In HPIP-b and HPIP-c, additional solvated structures resulting from hydrogen bonding through pyridyl nitrogen with solvent molecules are possible (Charts 2−4). Therefore, the molecules can have different solvated cluster structures which are in equilibrium. Their relaxation from the excited state can result in several decays. The observation of two lifetime decays could be due to superimposition of many such exponential decays.[53] Such behavior was observed in 2-(2′-aminophenyl)-benzimidazole.[54] In the dimethylamino group substituted analogue of HPIP-c, 2-(4′-*N*,*N*-dimethylaminophenyl)imidazo-[4,5-*c*]pyridine, it was found that the emission spectra shifted with excitation wavelength only in protic solvents due to the presence of different solvated structures.[55] As in HPBI, in nitrogen substituted analogues, the lifetime of the tautomer emission decreases strongly with an increase in temperature and the effect is marginal for the lifetime of the normal species. The significant change in decay of the tautomer with variation in temperature can be explained as follows. As discussed earlier, the torsional rotation of the tautomer to form a twisted ICT sate acts as a non-radiative channel for the tautomer. With an increase in temperature, the torsional rotation increases, which on the other hand enhances the non-radiative decay. This decreases the lifetime of the excited state tautomer. The decay times of the tautomer emissions of nitrogen substituted analogues are shorter than those of HPBI. This is consistent with the fact that the torsional rotation induced non-radiative decay increases upon substitution of nitrogen in the benzyl ring of HPBI.[31]

From the lifetimes obtained, Arrhenius plots are constructed. The quality of the linear fit can be determined by its regression (Figures 7 and 8). The decays of excited species follow an Arrhenius relation. The pre-exponential factor and activation energy are higher in tautomer emission than in normal emission (Table 5).

These results can be explained by the commonly accepted kinetics scheme for ESIPT exhibiting molecules (Scheme 1); i.e., the excited *cis*-enol undergoes the ESIPT process, while the excited *trans*-enol gives the normal emission. Increase in temperature affects the relative population of ground state conformers and increases the non-radiative decay which in turn affects the fluorescence of both enol and tautomer forms. Since the rise in temperature decreases the population of *cis*-enol and increases the non-radiative decay, the temperature effect is more pronounced for tautomer emission than that for normal emission.

4. CONCLUSION

The effects of temperature on the dual fluorescence of HPBI, HPIP-b, and HPIP-c due to ESIPT were studied in solvents of different polarity and hydrogen bonding capacity. Addition of hydrogen bonding solvent methanol molecules to form hydrogen bonded clusters is required along with the dielectric continuum and the clustering effect of the solvent in the solvation model IEF-PCM applied. The fluorescence ratio of the normal to tautomer band increases with an increase in temperature except for HPBI in methanol and ethylene glycol. This shows that the decrease in fluorescence with increase in temperature is greater in the tautomer band than in the normal band. The change in the fluorescence with increase in temperature is influenced by two factors: (i) the increase in the relative population of *trans*-enol with respect to that of *cis*-enol and (ii) the increase in non-radiative decay from the excited states. Since, with the rise in temperature, the population of *cis*-enol decreases and the non-radiative decay of tautomer increases, temperature affects the tautomer emission more than the normal emission. With a rise in temperature, the increase in non-radiative decay of the normal emission competes with the increase in relative population of *trans*-enol. Nitrogen substitution on the benzyl ring of HPBI increases the non-radiative deactivation to the ground state. The changes in the fluorescence emission are reflected in the lifetime of the normal and tautomer emissions. In general, the lifetime decreases with a rise in temperature, indicating the increase in the rate of non-radiative decay.

dx.doi.org/10.1021/jp405804c | J. Phys. Chem. B 2013, 117, 14079−14088

■ ASSOCIATED CONTENT

Supporting Information

Absorption, fluorescence, and fluorescence excitation spectra in different solvents at different temperatures, quantum yields, van't Hoff plots, decay profile, and population ratio plots. This material is available free of charge via the Internet at http://pubs.acs.org.

■ AUTHOR INFORMATION

Corresponding Author

*E-mail: gkrishna@iitg.ernet.in. Phone: +91-3612582315. Fax +91-3612582349.

Notes

The authors declare no competing financial interest.

■ ACKNOWLEDGMENTS

The authors thank Department of Science and Technology (DST), India, for the financial support and central instrumental facility (CIF), IIT Guwahati, for the time-resolved fluorescence measurements.

■ REFERENCES

(1) Efremov, R. G.; Baradaran, R.; Sazanov, L. A. The Architecture of Respiratory Complex I. *Nature* **2010**, *465*, 441−445.

(2) Ohnishi, T. Structural Biology: Piston Drives a Proton Pump. *Nature* **2010**, *465*, 428−429.

(3) Formosinho, S. J.; Arnaut, L. G. Excited-State Proton Transfer Reactions II. Intramolecular Reactions. *J. Photochem. Photobiol., A* **1993**, *75*, 21−48.

(4) Kwon, J. E.; Park, S. Y. Advanced Organic Optoelectronic Materials: Harnessing Excited-State Intramolecular Proton Transfer (ESIPT) Process. *Adv. Mater.* **2011**, *23*, 3615−3642.

(5) Chipem, F. A. S.; Mishra, A.; Krishnamoorthy, G. The Role of Hydrogen Bonding in Excited State Intramolecular Charge Transfer. *Phys. Chem. Chem. Phys.* **2012**, *14*, 8775−8790.

(6) Zhao, J.; Ji, S.; Chen, Y.; Guo, H.; Yang, P. Excited State Intramolecular Proton Transfer (ESIPT): From Principal Photophysics to the Development of New Chromophores and Applications in Fluorescent Molecular Probes and Luminescent Materials. *Phys. Chem. Chem. Phys.* **2012**, *14*, 8803−8817.

(7) Barbara, P. F.; Walsh, P. K. Picosecond Kinetic and Vibrationally Resolved Spectroscopic Studies of Intramolecular Excited-State Hydrogen Atom Transfer. *J. Phys. Chem.* **1989**, *93*, 29−34.

(8) Irie, M. Diarylethenes for Memories and Switches. *Chem. Rev.* **2000**, *100*, 1685−1716.

(9) Chou, P.-T.; Huang, C.-H.; Pu, S.-C.; Cheng, Y.-M.; Liu, Y.-H.; Wang, Y.; Chen, C.-T. Tuning Excited-State Charge/Proton Transfer Coupled Reaction via the Dipolar Functionality. *J. Phys. Chem. A* **2004**, *108*, 6452−6454.

(10) Celej, M. S.; Caarls, W.; Demchenko, A. P.; Jovin, T. M. A Triple-Emission Fluorescent Probe Reveals Distinctive Amyloid Fibrillar Polymorphism of Wild-Type α-Synuclein and Its Familial Parkinson's Disease Mutants. *Biochemistry* **2009**, *48*, 7465−7472.

(11) Chen, W.-H.; Xing, Y.; Pang, Y. A Highly Selective Pyrophosphate Sensor Based on ESIPT Turn-On in Water. *Org. Lett.* **2011**, *13*, 1362−1365.

(12) Zhang, G.; Wang, H.; Yu, Y.; Xiong, F.; Tang, G.; Chen, W. Optical Switching of 2-(2′-Hydroxyphenyl)benzoxazole in Different Solvents. *Appl. Phys. B: Lasers and Opt.* **2003**, *76*, 677−681.

(13) Paterson, M. J.; Robb, M. A.; Blancafort, L.; DeBellis, A. D. Mechanism of an Exceptional Class of Photostabilizers: A Seam of Conical Intersection Parallel to Excited State Intramolecular Proton Transfer (ESIPT) in *o*-Hydroxyphenyl-(1,3,5)-triazine. *J. Phys. Chem. A* **2005**, *109*, 7527−7537.

(14) Tang, K.-C.; Chang, M.-J.; Lin, T.-Y.; Pan, H.-A.; Fang, T.-C.; Chen, K.-Y.; Hung, W.-Y.; Hsu, Y.-H.; Chou, P.-T. Fine Tuning the Energetics of Excited-State Intramolecular Proton Transfer (ESIPT): White Light Generation in A Single ESIPT System. *J. Am. Chem. Soc.* **2011**, *133*, 17738−17745.

(15) Lim, S.-J.; Seo, J.; Park, S. Y. Photochromic Switching of Excited-State Intramolecular Proton-Transfer (ESIPT) Fluorescence: A Unique Route to High-Contrast Memory Switching and Non-destructive Readout. *J. Am. Chem. Soc.* **2006**, *128*, 14542−14547.

(16) Mosquera, M.; Penedo, J. C.; Rodríguez, M. C. R.; Rodríguez-Prieto, F. Photoinduced Inter- and Intramolecular Proton Transfer in Aqueous and Ethanolic Solutions of 2-(2′-Hydroxyphenyl)-benzimidazole: Evidence for Tautomeric and Conformational Equilibria in the Ground State. *J. Phys. Chem.* **1996**, *100*, 5398−5407.

(17) Douhal, A.; Amat-Guerri, F.; Lillo, M. P.; Acuña, A. U. Proton Transfer Spectroscopy of 2-(2′-Hydroxyphenyl)imidazole and 2-(2′-Hydroxyphenyl)benzimidazole Dyes. *J. Photochem. Photobiol., A* **1994**, *78*, 127−138.

(18) Vázquez, S. R.; Rodríguez, M. C. R.; Rodríguez-Prieto, M. M. F. Excited-State Intramolecular Proton Transfer in 2-(3′-Hydroxy-2′-pyridyl)benzoxazole. Evidence of Coupled Proton and Charge Transfer in the Excited State of Some *o*-Hydroxyarylbenzazoles. *J. Phys. Chem. A* **2007**, *111*, 1814−1826.

(19) Sinha, H. K.; Dogra, S. K. Ground and Excited State Prototropic Reactions in 2-(*o*-Hydroxyphenyl)benzimidazole. *Chem. Phys.* **1986**, *102*, 337−347.

(20) Roberts, E. L.; Dey, J.; Warner, I. M. Excited-State Intramolecular Proton Transfer of 2-(2′-Hydroxyphenyl)benzimidazole in Cyclodextrins and Binary Solvent Mixtures. *J. Phys. Chem. A* **1997**, *101*, 5296−5301.

(21) del Valle, J. C.; Claramunt, R. M.; Catalán, J. Fluorescence Spectroscopy and Amplified Spontaneous Emission (ASE) of Phenylimidazoles: Predicted Vibronic Coupling Along the Excited-State Intramolecular Proton Transfer in 2-(2′-Hydroxyphenyl)-imidazoles. *J. Phys. Chem. A* **2008**, *112*, 5555−5565.

(22) Henary, M. M.; Wu, Y.; Cody, J.; Sumalekshmy, S.; Li, J.; Mandal, S.; Fahrni, C. J. Excited-State Intramolecular Proton Transfer in 2-(2′-Arylsulfonamidophenyl)benzimidazole Derivatives: The Effect of Donor and Acceptor Substituents. *J. Org. Chem.* **2007**, *72*, 4784−4797.

(23) Cheng, Y.-M.; Pu, S.-C.; Hsu, C.-J.; Lai, C.-H.; Chou, P.-T. Femtosecond Dynamics on 2-(2′-Hydroxy-4′-diethylaminophenyl)-benzothiazole: Solvent Polarity in the Excited-State Proton Transfer. *ChemPhysChem* **2006**, *7*, 1372−1381.

(24) Kim, Y. H.; Roh, S.-G.; Jung, S.-D.; Chung, M.-A.; Kim, H. K.; Cho, D. W. Excited-State Intramolecular Proton Transfer on 2-(2′-Hydroxy-4′-R-phenyl)benzothiazole Nanoparticles and Fluorescence Wavelength Depending on Substituent and Temperature. *Photochem. Photobiol. Sci.* **2010**, *9*, 722−729.

(25) Mordziński, A.; Grabowska, A. Intramolecular Proton Transfer in Excited Benzoxazoles. *Chem. Phys. Lett.* **1982**, *90*, 122−127.

(26) Barbara, P. F.; Brus, L. E.; Rentzepis, P. M. Intramolecular Proton Transfer and Excited-State Relaxation in 2-(2-Hydroxyphenyl)-benzothiazole. *J. Am. Chem. Soc.* **1980**, *102*, 5631−5635.

(27) Al-Soufi, W.; Grellmann, K. H.; Nickel, B. Triplet State Formation and *cis*→*trans* Isomerization in the Excited Singlet State of the Keto Tautomer of 2-(2′-Hydroxyphenyl)benzothiazole. *Chem. Phys. Lett.* **1990**, *174*, 609−616.

(28) Brewer, W. E.; Martinez, M. L.; Chou, P.-T. Mechanism of the Ground-State Reverse Proton Transfer of 2-(2-Hydroxyphenyl)-benzothiazole. *J. Phys. Chem.* **1990**, *94*, 1915−1918.

(29) Stephan, J. S.; Grellmann, K. H. Photoisomerization of 2-(2′-Hydroxyphenyl)benzoxazole. Formation and Decay of the Trans-Keto Tautomer in Dry and in Water-Containing 3-Methylpentane. *J. Phys. Chem.* **1995**, *99*, 10066−10068.

(30) Nagaoka, S.; Itoh, A.; Mukai, K.; Nagashima, U. Investigation of Triplet States of 2- (2′-Hydroxyphenyl)benzothiazole and 2-(2′-Hydroxypbenyl)benzoxazole by Transient Absorption Spectroscopy and ab Initio Calculations. *J. Phys. Chem.* **1993**, *97*, 11385−11392.

(31) Chipem, F. A. S.; Krishnamoorthy, G. Comparative Theoretical Study of Rotamerism and Excited State Intramolecular Proton

Transfer of 2-(2′-Hydroxyphenyl)benzimidazole, 2-(2′-Hydroxyphenyl)imidazo[4,5-*b*]pyridine, 2-(2′-Hydroxyphenyl)-imidazo[4,5-*c*]pyridine and 8-(2′-Hydroxyphenyl)purine. *J. Phys. Chem. A* **2009**, *113*, 12063−12703.
(32) Chipem, F. A. S.; Dash, N.; Krishnamoorthy, G. Role of Nitrogen Substitution in Phenyl Ring on Excited State Intramolecular Proton Transfer and Rotamerism of 2-(2′-Hydroxyphenyl)-benzimidazole: A Theoretical Study. *J. Chem. Phys.* **2011**, *134*, 104308-1−104308-9.
(33) Brenlla, A.; Veiga, M.; Lustres, J. L. P.; Rodríguez, M. C. R.; Rodríguez-Prieto, F.; Mosquera, M. Photoinduced Proton and Charge Transfer in 2-(2′-Hydroxyphenyl)imidazo[4,5-*b*]pyridine. *J. Phys. Chem. B* **2013**, *117*, 884−896.
(34) Konoshima, H.; Nagao, S.; Kiyota, I.; Amimoto, K.; Yamamoto, N.; Sekine, M.; Nakata, M.; Furukawa, K.; Sekiya, H. Excited-State Intramolecular Proton Transfer and Charge Transfer in 2-(2′-Hydroxyphenyl)benzimidazole Crystals Studied by Polymorphs-Selected Electronic Spectroscopy. *Phys. Chem. Chem. Phys.* **2012**, *14*, 16448−16457.
(35) Krishnamoorthy, G.; Dogra, S. K. Excited State Intramolecular Proton Transfer in 2-(2′-Hydroxyphenyl)-3*H*-imidazo[4,5-*b*]pyridine: Effect of Solvents. *J. Lumin.* **2001**, *92*, 91−102.
(36) Krishnamoorthy, G.; Dogra, S. K. Prototropic Reactions of 2-(2′-Hydroxyphenyl)-3*H*-imidazo[4,5-*b*]pyridine in Aqueous and Organic Solvents. *J. Lumin.* **2001**, *92*, 103−114.
(37) Balamurali, M. M.; Dogra, S. K. Excited State Intramolecular Proton Transfer in 2-(2′-Hydroxyphenyl)-1*H*-imidazo[4,5-*c*]pyridine: Effects of Solvents. *J. Photochem. Photobiol., A* **2002**, *154*, 81−92.
(38) Rettig, W. Charge Separation in Excited States of Decoupled Systems—TICT Compounds and Implications Regarding the Development of New Laser Dyes and the Primary Process of Vision and Photosynthesis. *Angew. Chem., Int. Ed. Engl.* **1986**, *25*, 971−988.
(39) Kawski, A.; Kukliński, B.; Bojarski, P. Temperature Influence on Dual Fluorescence of 4-(Dimethylamino)benzaldehyde in 1,2-Dichloroethane and Ethyl Acetate. *Chem. Phys. Lett.* **2008**, *455*, 52−54.
(40) Wohlfarth, C. Permittivity (Dielectric Constant) of Liquids. In *CRC Handbook of Chemistry and Physics*, 91st ed.; Haynes, W. M., Ed.; CRC Press, Taylor & Francis Group, New York, 2010; Section 6, pp 186−207.
(41) *Refractive Indices of Pure Liquids and Binary Liquids Mixtures (Supplement to III/38)*; Book Series: Landolt-Börnstein − Group III Condensed Matter; Springer: Berlin, Heidelberg, 2008; Vol. *47*, DOI: 10.1007/978-3-540-75291-2.
(42) Miertuš, S.; Scrocco, E.; Tomasi, J. Electrostatic Interaction of A Solute With A Continuum. A Direct Utilization of Ab Initio Molecular Potentials for the Prevision of Solvent Effects. *Chem. Phys.* **1981**, *55*, 117−129.
(43) Cancès, E.; Mennucci, B.; Tomasi, J. A New Integral Equation Formalism for the Polarizable Continuum Model: Theoretical Background and Applications to Isotropic and Anisotropic Dielectrics. *J. Chem. Phys.* **1997**, *107*, 3032−3041.
(44) Hohenberg, P.; Kohn, W. Inhomogeneous Electron Gas. *Phys. Rev. B* **1964**, *136*, 864−871.
(45) Kohn, W.; Sham, L. J. Self-Consistent Equations Including Exchange and Correlation Effects. *Phys. Rev. A* **1965**, *140*, 1133−1138.
(46) Becke, A. D. Density Functional Thermochemistry. III. The Role of Exact Exchange. *J. Chem. Phys.* **1993**, *98*, 5648−5652.
(47) Lee, C.; Yang, W.; Parr, R. G. Development of the Colle-Salvetti Correlation-Energy Formula Into A Functional of the Electron Density. *Phys. Rev. B* **1988**, *37*, 785−789.
(48) Frisch, M. J.; Trucks, G. W.; Schlegel, H. B.; Scuseria, G. E.; Robb, M. A.; Cheeseman, J. R.; Montgomery, J. A. Jr.; Vreven, T.; Kudin, K. N.; Burant, J. C.; et al. *Gaussian 03*, revision E.01; Gaussian, Inc.: Wallingford, CT, 2004.
(49) Das, K.; Sarkar, N.; Ghosh, A. K.; Majumdar, D.; Nath, D. N.; Bhattacharyya, K. Excited-State Intramolecular Proton Transfer in 2-(2′-Hydroxyphenyl)benzimidazole and -benzoxazole: Effect of Rotamerism and Hydrogen Bonding. *J. Phys. Chem.* **1994**, *98*, 9126−9132.
(50) Dupradeau, F. Y.; Case, D. A.; Yu, C. Z.; Jimenez, R.; Romesberg, F. E. Differential Solvation and Tautomer Stability of a Model Base Pair within the Minor and Major Grooves of DNA. *J. Am. Chem. Soc.* **2005**, *127*, 15612−15617.
(51) Brenlla, A.; Veiga, M.; Rodríguez, M. C. R.; Mosquera, M.; Rodríguez-Prieto, F. Fluorescence of Methylated Derivatives of Hydroxyphenylimidazopyridine. Resolution of Strongly Overlapping Spectra and A New ESIPT Dye Showing Very Efficient Radiationless Deactivation. *Photochem. Photobiol. Sci.* **2011**, *10*, 1622−1636.
(52) Kim, Y.; Yoon, M.; Kim, D. Excited-State Intramolecular Proton Transfer Coupled-Charge Transfer of *p*-*N*,*N*-Dimethylaminosalicylic Acid in Aqueous β-Cyclodextrin Solutions. *J. Photochem. Photobiol., A* **2001**, *138*, 167−175.
(53) James, D. R.; Ware, W. R. A Fallacy in the Interpretation of Fluorescence Decay Parameters. *Chem. Phys. Lett.* **1985**, *120*, 455−459.
(54) Santra, S.; Dogra, S. K. Excited-State Intramolecular Proton Transfer in 2-(2′-Aminophenyl)benzimidazole. *Chem. Phys.* **1998**, *226*, 285−296.
(55) Krishnamoorthy, G.; Dogra, S. K. Dual Fluorescence of 2-(4′-*N*,*N*-Dimethylaminophenyl)pyrido[3,4-*d*]imidazole: Effect of Solvents. *Spectrochim. Acta, Part A* **1999**, *55*, 2647−2658.